Shell variability of *Pseudocubus obeliscus* Haeckel in the early autumn radiolarian fauna off Tassha, Sado Island, central Japan

Toshiyuki KURIHARA* and Atsushi MATSUOKA*

Abstract

Shell variability of *Pseudocubus obeliscus* Haeckel within the early autumn radiolarian fauna collected from the Sea of Japan, off Tassha, Sado Island in 2001 is demonstrated based on detailed scanning electron microscopic observations and comparisons among morphologically varied specimens. *Pseudocubus obeliscus* has an inverted truncated-pyramidal skeleton consisting of an initial spicule, rings formed by several arches, columellae, and other secondary spines. The initial spicule is comprised of a median bar, an apical spine, a dorsal spine, two primary lateral spines, and an axial spine. The ventral spine and secondary lateral spines are absent. Comparative observations of morphologically varied specimens with reference to highly symmetrical, well-regulated specimens show that morphologic variation in *P. obeliscus* is caused by the transformation of angles between columellae and a primary ring, shape of the primary ring and columellae, and their combination. In addition, some secondary arches are formed for rebuilding a distorted pyramidal skeleton. Therefore, it is concluded that shell variability is expressed by the skeletal instability of some specific parts and self-organizing formation of secondary arches.

Key words: *Pseudocubus obeliscus*, Radiolaria, Sado Island, Sea of Japan, shell variability.

Introduction

Appropriate recognition of intraspecific variation in shell morphology of Polycystine Radioalria is fundamentally linked to its biosystematics, because since Haeckel's (1887) study, the classification scheme has been based completely on the geometric arrangement of

---

* Department of Geology, Faculty of Science, Niigata University, Niigata 950-2181, Japan
(Manuscript received 24 January, 2005; accepted 3 March, 2005)

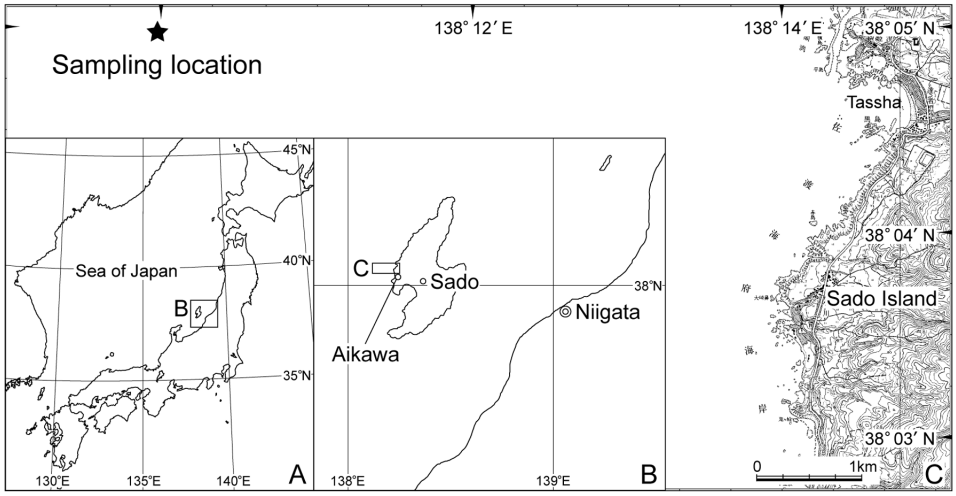

Fig. 1. Index map showing the sampling location (star symbol). The topography is from the 1:25,000 scale "Aikawa" map sheet published by the Geographical Survey Institute of Japan.

skeletal elements. In fossil materials, the judgment of whether shell variation is intraspecific or interspecific cannot be directly supported by other biological evidence, so it often becomes subjective and depends largely on the practical experience of individual researchers. Recently, morphological distinctions resulting from skeletal growth have been addressed in several species (Anderson and Bennett, 1985; Anderson et al., 1986; Swanberg and Bjørklund, 1987; Matsuoka, 1992) using laboratory cultures and the morphometry of variably-sized specimens collected from plankton tow samples. Knowledge accumulated from these studies can be very helpful to the refinement of taxonomies for fossil radiolarians. Similar studies should be applied to other various living taxa to clarify the range of shell variability, but unfortunately few studies are available due to the technical difficulties involved in living radiolarian research.

Since introduction of research boat "IBIS2000" to the Sado Marine Biological Station, living radiolarian studies of the Sea of Japan have continued by the second author (A.M.) and his collaborators (Matsuoka et al., 2001, 2002; Itaki et al., 2003; Kurihara and Matsuoka, 2004). We can now obtain information about changing seasonal radiolarian faunal compositions in the seawater off Tassha, Sado Island. A plankton tow sample collected on September 26 in 2001 contained numerous plagiacanthid and lophophaenid nassellarians. This fauna includes *Pseudocubus obeliscus* Haeckel, a spicular nassellarian, which is highly variable morphologically. We describe the basic skeletal structure and morphologic variation of this species. Radiolarian faunal data from the early autumn in 2001 are also briefly reported.

Table 1. List of early autumn radiolarian species from sea water off Tassha, Sado Island.

NASSELLARIA	SPUMELLARIA
Litharachnium tentorium Haeckel	*Dictyocoryne* sp.
Neosemantis distephanus Popofsky	*Euchitonia* aff. *elegans* (Ehrenberg)
Neosemantis ? sp.	*Hexacontium* sp.
?*Peridium longispinum* Jørgensen	*Larcospina quadrangular* Haeckel
Phormacantha hystrix (Jørgensen)	*Spongosphaera streptacantha* Haeckel
Plectacantha trichoides Jørgensen	*Tetrapyle octacantha* Müller
Plectacantha oikiskos (Jørgensen)	
Plectacantha sp. A	
Plectacantha sp. B	
Plectacantha ? sp.	
Pseudocubus obeliscus Haeckel	
Pseudocubus sp. A	
Pseudodictyophimus gracilipes (Bailey)	

Materials and methods

Plankton samples were collected from sea water of 200-0 m at a location approximately 6 km west of Tassha, Sado City (former name: Aikawa Town), Sado Island, Niigata Prefecture, central Japan (Fig. 1). Sampling was conducted on the morning of September 26, 2001 when eight samples were obtained, using a 100μm opening net.

The plankton sample used here (926-2SD-5, depth: 200-0 m) was placed in ca. 50% sulfuric acid for a day to eliminate the organic matter from radiolarian specimens. Following this process, residues were rinsed in water and kept in an aqueous ethanol solution. Over 180 radiolarian specimens were picked from dried residues and mounted on stubs for observation by scanning electron microscope (SEM, JEOL JSM-5600).

Brief overview of radiolarian fauna

Radiolarian species obtained from sample 926-2SD-5 are listed in Table 1; SEM images of representative species are illustrated on Plates 1 and 2. The fauna is characterized by the abundant occurrence of nassellarians belonging to the families Plagiacanthidae and Lophophaenidae. These families include the following species: *Neosemantis distephanus* Popofsky (Pl. 1, fig. 1), *Pseudocubus obeliscus* (Pl. 1, fig. 3), *Plectacantha trichoides* Jørgensen (Pl. 1, fig. 6), *Plectacantha oikiskos* (Jørgensen) (Pl. 1, fig. 8), ?*Peridium*

Table 2. List showing definitions and abbreviations of skeletal elements.

abbreviation	definition
MB	median bar
A	apical spine
D	dorsal spine
L	primary lateral spine
Lr	right **L**
Ll	left **L**
AX	axial spine
V	ventral spine
l	secondary lateral spine
PR	proximal ring
DR	distal ring
D'	lateral branch of **D**
l'	laterally directed spine arising from diametrically opposite apex of **L**
l'r	right **l'**
l'l	left **l'**
A'	laterally directed spine arising from the junction of **A** and **PR**
V'	laterally directed spine arising from the ventral apex of **PR**
AC	apical columella
l'C	columella arising from the junction of **l'** and **PR**
l'Cr	right **l'C**
l'Cl	left **l'C**
VC	ventral columella

longispinum Jørgensen (Pl. 1, fig. 9), *Phormacantha hystrix* (Jørgensen) (Pl. 2, fig. 2), and *Pseudodictyophimus gracilipes* (Bailey) (Pl. 2, fig. 1). In addition to these species, specimens having a very fragile skeleton, which probably belong to *Plectacantha* (Pl. 1, figs. 5, 7), are frequently present. Spumellarians also commonly occur e.g., *Spongosphaera streptacantha* Haeckel (Pl. 2, fig. 8), and pyloniid species including *Tetrapyle octacantha* Müller (Pl. 2, figs. 4, 5) and *Larcospina quadrangular* Haeckel (Pl. 2, fig. 6) are especially dominant in the fauna.

According to Matsuoka et al. (2001), the late summer (early September) fauna of 2000, obtained 2-3 km west off Tassha, contains dominantly *Didymocyrtis tetrathalamus tetrathalamus* (Haeckel), *Tetrapyle octacantha*, *Zygocircus productus* (Hertwig), *Neosemantis distephanus*, *Lophophaena hispida* (Ehrenberg), and *Pseudocubus obeliscus*. This fauna differs slightly from the early autumn radiolarian fauna of 2001 in spumellarian species composition. Concerning nassellarians, however, both faunas are similar in terms of dominating plagiacanthid and lophophaenid species.

Basic skeletal structure of *Pseudocubus obeliscus*

Before discussing the shell variability of *Pseudocubus obeliscus*, we must first clarify its basic skeletal structure. Descriptive terms for the nassellarian skeleton (**MB**, **A**, **D**, **L**, **AX**, **V**)

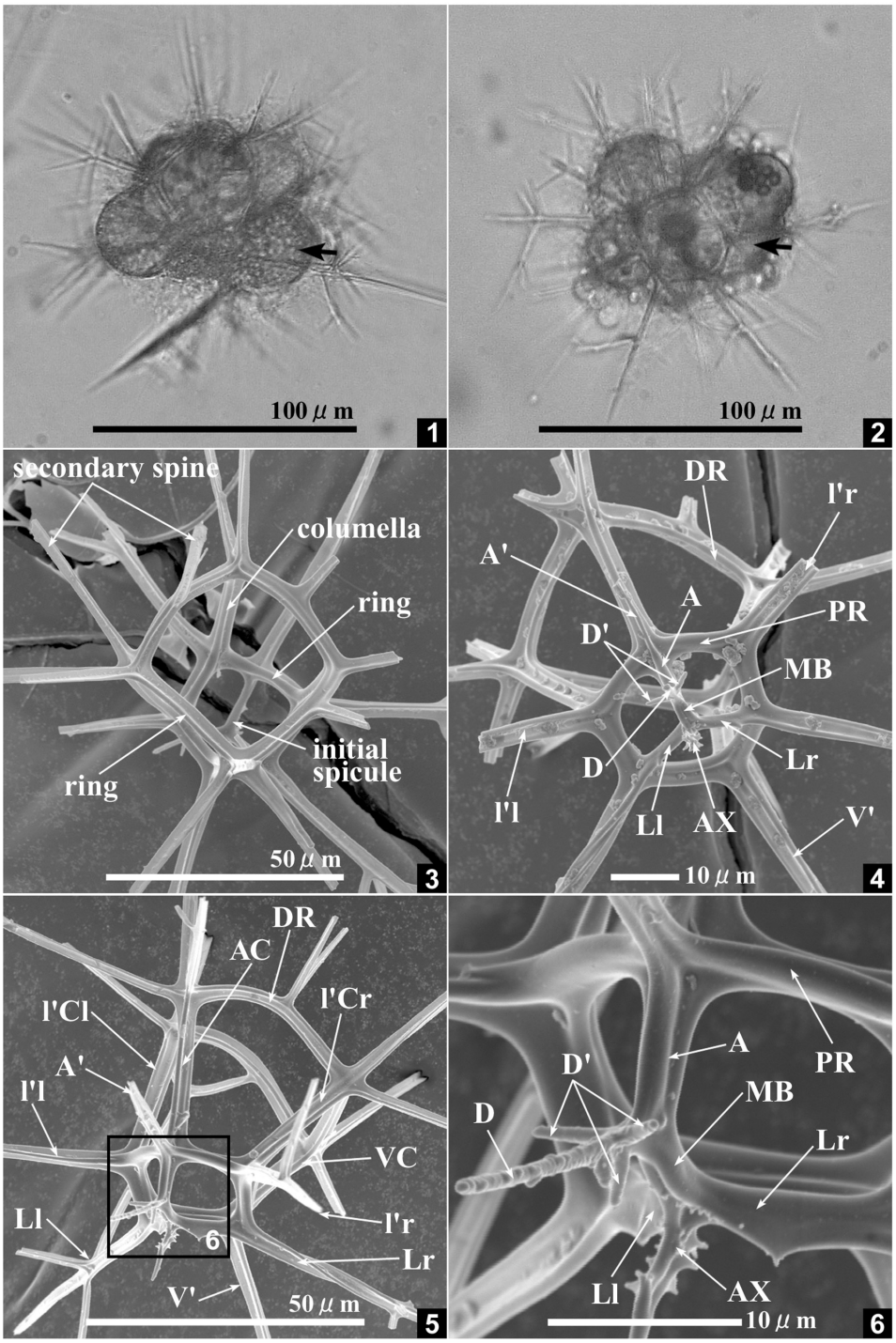

Fig. 2. Light microscopic and SEM images showing the living body and skeletal structure of *Pseudocubus obeliscus* Haeckel. 1, 2: Light microscopic images showing the living body of *P. obeliscus*. 1: ID number=20020904_3018_01_d1_ma, lateral view, 2: ID number=20020905_2848_02_d1_ms, apical view. 3-6: SEM images showing the skeletal structure of *P. obeliscus*. 3: ID number=926-2SD-5, 741-4-10, apical view, 4: ID number=926-2SD-5, 741-4-1, basal view, 5, 6: ID number=926-2SD-5, 742-5-6, oblique basal view. See Table 2 for abbreviations of skeletal elements.

follow Petrushevskaya (1968), De Wever et al. (1979), and Dumitrica (1991). Some special terms (**D'**, **PR**, **l'**, **A'**, **V'**, **DR**) produced by Sugiyama (1993) are also used below. Abbreviations of all descriptive terms used in this paper are listed in Table 2.

The skeleton of *Pseudocubus obeliscus* consists of a nassellarian initial spicule, arches (= skeletal material connecting two spines), rings (formed by the connection of several arches), longitudinal spines (= columellae) arising from the initial spicule and rings, and other secondary spines (Fig. 2-3). Each skeletal element is described in detail in the following section. These elements make up an inverted truncated-pyramidal skeletal framework that corresponds to a cephalis in the skeletal classification of Nassellaria. This species completely lacks a cephalic shell wall and other segments (thorax, abdomen, etc.). As shown in Figs. 2-1 and 2-2, the central capsule (black arrow in the figure), which is expressed by a transparent orange mass pinched in four portions in the living specimen, is situated in and around the cephalis and is supported by the inverted pyramidal skeletal framework.

The initial spicule is comprised of the following elements: a median bar (**MB**), an apical spine (**A**), a dorsal spine (**D**), two primary lateral spines (**Lr**: right primary lateral spine, **Ll**: left primary lateral spine), and an axial spine (**AX**). In addition, **D** has thinner and shorter three lateral branches (**D'**) in its proximal portion (Figs. 2-4 and 2-6). A ventral spine (**V**) and secondary lateral spines (**l**), which are the primary elements in the nassellarian initial spicule, are absent in all our specimens. **MB**, **A**, and **L** are shallowly grooved. **AX** is also shallowly grooved but thinner than **MB**, **A**, and **L** and tapers distally with several conical projections in the proximal portion (Fig. 2-6). **D** and **D'** are thinner than other initial spicule elements, circular in cross section, and taper distally.

Spines **A**, **Lr**, and **Ll** branch laterally to form three arches connected to each other on the same horizontal plane above **MB**. This connection makes a hexagonal ring, called a proximal ring (**PR**) (Fig. 2-4). From the apexes of the hexagonal **PR**, six spines radiate horizontally or slightly downward (Figs. 2-4 and 2-5). Two are direct extensions of **Lr** and **Ll**. Stout, three-bladed spines (**l'r** and **l'l**) arise from diametrically opposite apexes to both the **L** apexes. The other two spines are **A'** and **V'**, which arise from the junction of **A** and **PR** and the ventral apex of **PR**, respectively. The direct extensions of **Lr** and **Ll**, **l'r**, **l'l**, **A'**, and **V'** have almost the same morphology, gently taper distally, and commonly have two or three branches in the middle.

Longitudinal spines forming four sides of the inverted pyramidal framework are stout and three-bladed, and are described as "columellae (singular form: columella)" herein. They arise at angles of 70 to 80 degrees to the **PR** plane. Four columellae are classified into an apical columella (**AC**), two **l'** columellae (**l'Cr**, **l'Cl**), and a ventral columella (**VC**) based on their positions; **AC** directly extends from **A** through the junction of **A** and **PR**, and **l'C** and **VC** arise from the same junctions of **l'** and **V'** with **PR**, respectively (Fig. 2-5). Adjacent columellae are connected by three-bladed arches. These arches form a distal ring (**DR**) (Figs. 2-4 and 2-5); they are convex upward and have a rather thin spine extending in the apical direction. From each junction of a columella with **DR**, one or two secondary spines radiate in the lateral direction.

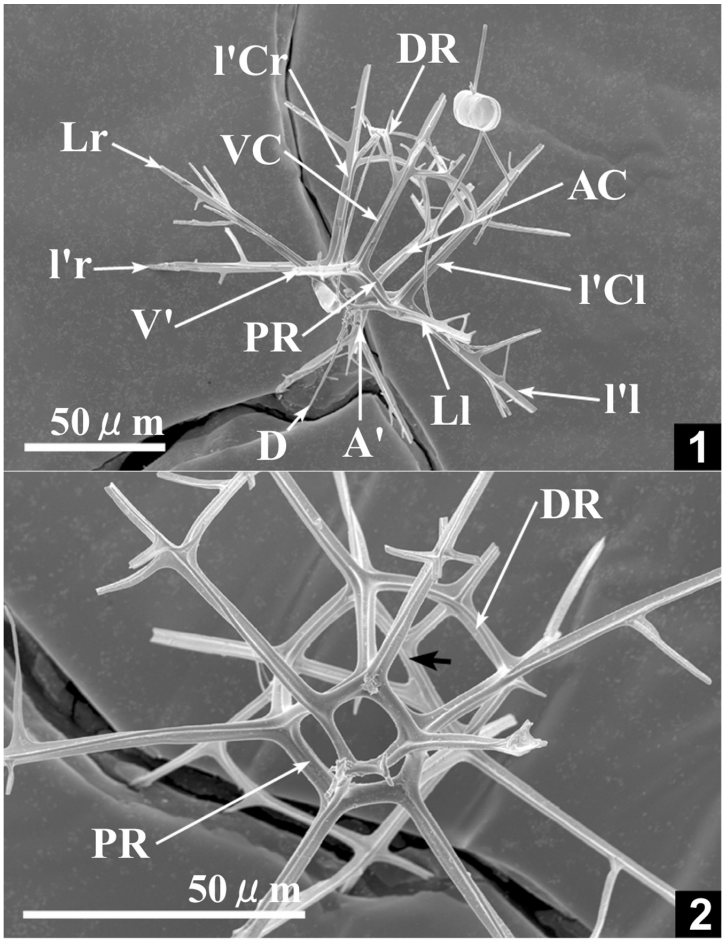

Fig. 3. SEM images showing *Pseudocubus obeliscus* in various growth stages. 1: ID number=926-2SD-5, 742-1-9, oblique lateral view, 2: ID number=926-2SD-5, 742-1-7, oblique basal view. See Table 2 for abbreviations of skeletal elements.

Shell variability in *Pseudocubus obeliscus*

In the preceding paragraph, we discussed the basic skeletal structure of *Pseudocubus obeliscus* by taking highly symmetrical, well-regulated, and probably immature specimens for descriptive purposes. However, these specimens as shown in Fig. 2 are less common. In actuality, morphologically varied specimens are more abundant and their variation is caused by the

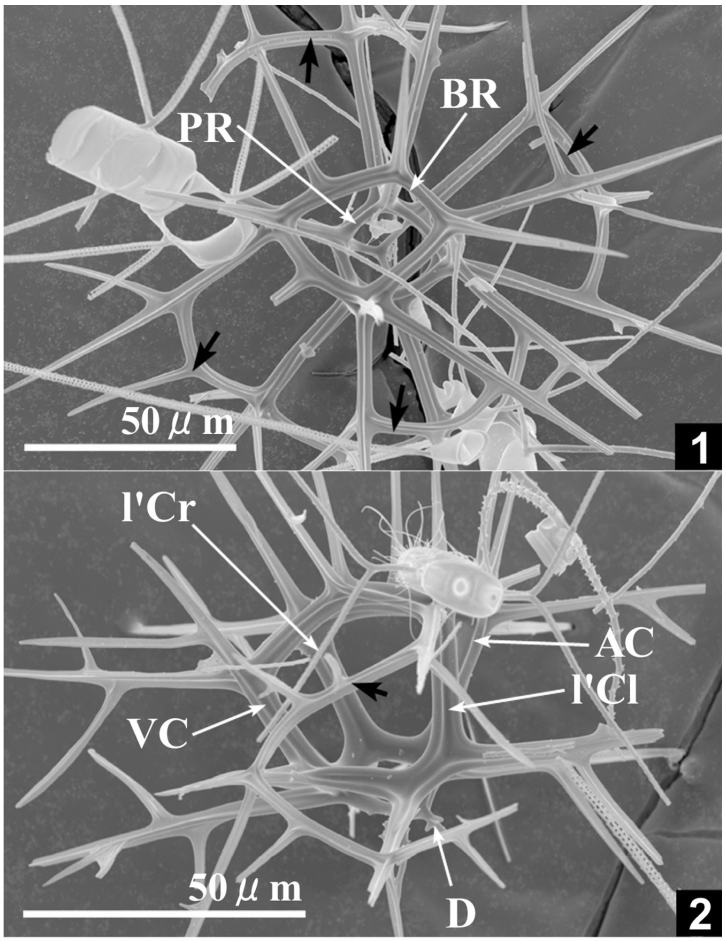

Fig. 4. SEM images showing *Pseudocubus obeliscus* in various growth stages. 1: ID number=926-2SD-5, 743-2-8, apical view, 2: ID number=926-2SD-5, 743-6-3, lateral view. See Table 2 for abbreviations of skeletal elements.

following two factors: (1) differing growth stages, (2) displacement or deformation of skeletal elements with reference to those of the morphologically well-regulated specimens. Based on previous morphogenetic studies (Anderson and Bennett, 1985; Anderson et al., 1986; Swanberg and Bjørklund, 1987; Matsuoka, 1992), the former can be recognized by the increasing length of spines, presence of additional skeletal elements, etc. The latter is attributed to the unstable location or form of skeletal elements. Although the term "shell variability" is used here for describing the morphological variation, it is important to appreciate the growth process of *P. obeliscus* before examining its shell variability. So, first we explain skeletal

development by the growth process, then discuss the pattern of shell variability based on detailed SEM observations of several morphologically characteristic specimens.

Skeletal development by growth process: In the four specimens shown on Figs. 3 and 4, the fundamental skeletal elements except for **DR** are relatively consistent in shape and arrangement. In the specimen shown in Fig. 3-1, **DR**-forming arches are thinner than other skeletal elements. Other mature specimens (Figs. 3-2, 4-1, 4-2) have **DR**-forming arches that are similar to columellae in thickness, providing evidence that **DR** develops subsequent to the formation of an initial spicule, **PR**, and columellae. In the specimen shown in Fig. 3-2, arches connecting apexes of **DR** are present above the **DR** plane (black arrow in the figure). Similar arches originating from branches of **L**, **A'**, **V'**, **l'**, and other outward-extending secondary spines express varying degrees of development and are commonly observed (black arrows in Figs. 4-1, 4-2). In addition, thickening of spines represented by well-developed ridges and deep grooves (Fig. 4-2) and increasing spine length are obviously important processes for skeletal growth.

The skeletal growth pattern after the construction of fundamental elements (initial spicule, proximal ring, columella) is characterized as follows, in random order: (1) formation of **DR**, (2) outward extension of **L**, **A'**, **V'**, **l'**, columellae, and secondary spines arising from **DR**, (3) buildup of arches on **DR**, (4) branching and arching of **L**, **A'**, **V'**, **l'**, and other secondary spines, (5) thickening of spines. As shown in Figs. 2-1, 2-2, the shell of this species is likely to support its central capsule in some way. Thus, it is possible that accretional skeletal growth develops progressively with the increasing the volume of the central capsule.

Shell variability: Based on observations of several specimens, we conclude that variation of the external skeletal morphology is mainly attributable to the following transformations of skeletal elements: (1) angles between columellae and a **PR** plane, (2) shape of **PR**, (3) bending of columellae, and (4) combination of factors all above.

The specimen shown in Fig. 5-1 is a prime example of (1). This specimen does not lose shape so much, but **AC** is radiating at a very low angle to the **PR** plane. Normally, **DR** connects four columellae and makes a quadrangular shape in apical view, but **DR** of this specimen expresses a distorted triangular shape. Specimen Fig. 5-2 is an interesting example of (2). Usually **V'** and **VC** arise from the same apex of **PR**. In this specimen, however, the **PR**-forming arch arising from **Lr** bifurcates: one branch extends in the apical direction as **VC**, and the other radiates laterally as **V'**. The arch arising from **Ll** connects only to **V'**. As shown in the next example (Fig. 6-1), **PR**-forming arches in the ventral side tend to be morphologically unstable compared with other **PR**-forming elements, i.e., morphological variation caused by the combination of (1) and (2). In this specimen, **AC** radiates obliquely upward at an angle of 30 degrees, and the **PR**-forming arches on the ventral side, indicated by the black arrow (a), protrude from **L** at a very high angle. Consequently the pyramidal framework tilts toward the dorsal side. Generally, variation of the interval between adjacent columellae resulting from (1) and (2) has a critical influence on the shape of **DR**. For example, in the specimen shown on

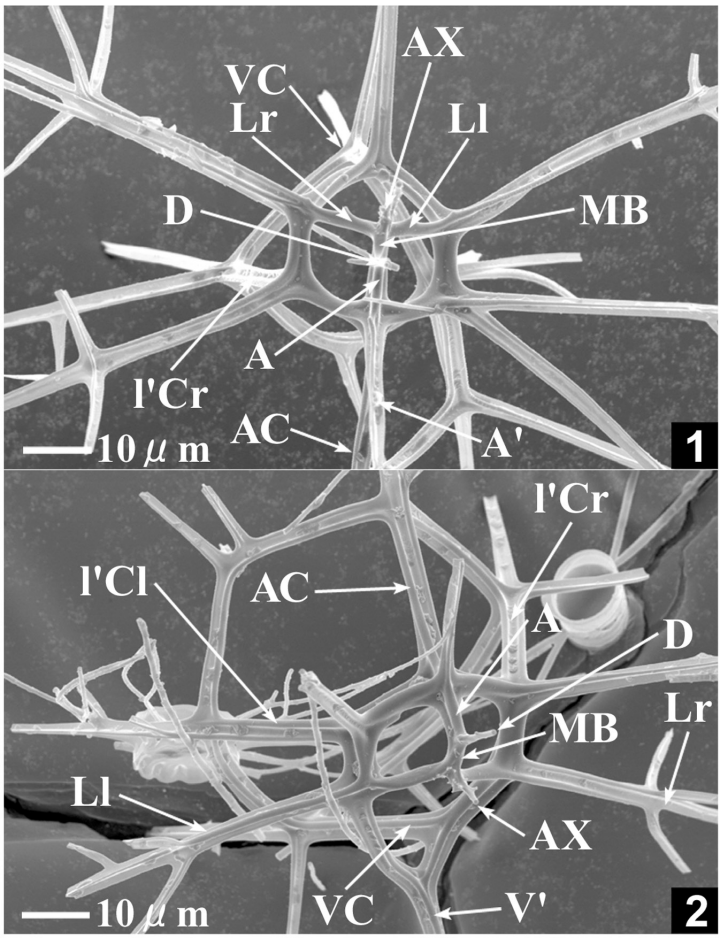

Fig. 5. SEM images showing the morphologic variability of *Pseudocubus obeliscus*. 1: ID number=926-2SD-5, 741-2-7, basal view, 2: ID number=926-2SD-5, 741-5-2, oblique basal view. See Table 2 for abbreviations of skeletal elements.

Fig. 6-1, the junction on **DR** between **VC** and **l'Cr**, indicated by the black arrow (b), was probably formed for adjusting the distorted pyramidal shape. Example (3) is illustrated on Fig. 6-2. The columellae of this specimen trend inward and do not make a pyramidal framework.

The shell variability mentioned above is mainly caused by slight transformations of skeletal elements such as the angle of columellae and shape of **PR** during the early ontogenic stage. The well-regulated shell shape with high cubic symmetry (Fig. 2) is believed to provide the most stable and efficient shape for supporting the central capsule. However, if the skeletal

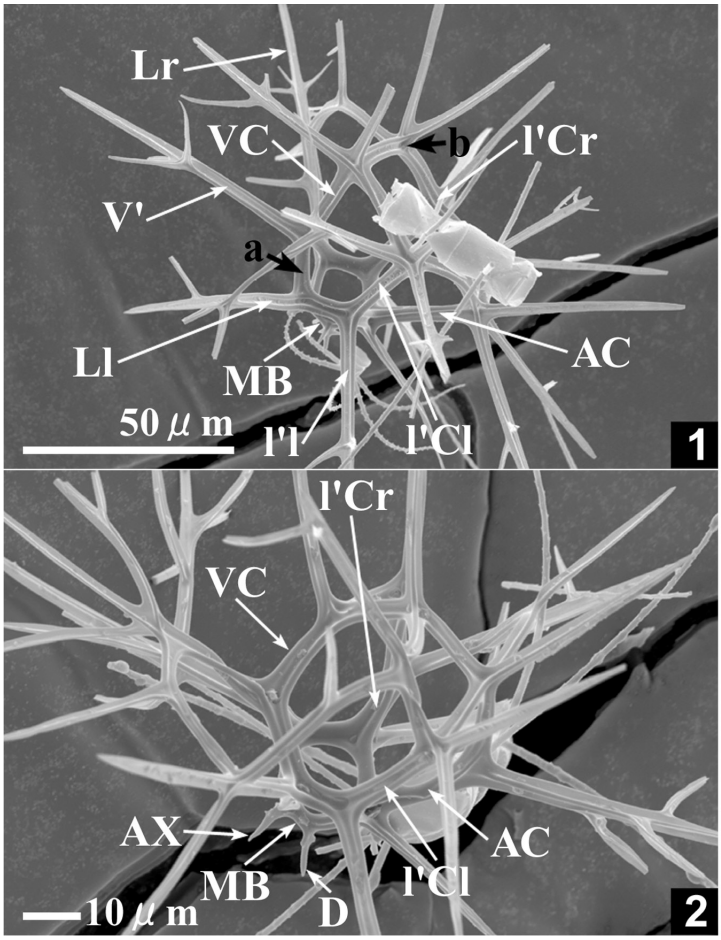

Fig. 6. SEM images showing the morphologic variability of *Pseudocubus obeliscus*. 1: ID number=926-2SD-5, 741-1-7, oblique lateral view, 2: ID number=926-2SD-5, 743-3-1, oblique lateral view. See Table 2 for abbreviations of skeletal elements.

elements are not formed ideally, the formation of more flexible secondary arches compensates for the distortion of whole shape, as shown in Fig. 6-1. The shell variability of this species depends largely on the morphological instability of specific skeletal elements, which strongly relates to the importance of ontogenic order, and the self-organizing formation of secondary arches.

The morphologic variation in *Pseudocubus obeliscus* is determined to be intraspecific variation because morphologically stable and unstable parts reflecting skeletogenesis are easily

recognized as discussed above. In addition, all specimens examined here are completely sympatric. However, in fossil radiolarian species, it is common for specimens having slightly different morphologies to be identified as different species. This type of problem is subjective and can never be proven by fossil evidence alone. Living species can provide substantial information not only about shell shape but also ecology and molecular biology. We should extend our biosystematic knowledge of a greater number of living taxa in order to better examine the fossil classification.

Acknowledgments

Prof. M. Nozaki at the Sado Marine Biological Station, Niigata University, allowed us use of facilities in the station. We would like to thank Drs. E.S. Carter and H. Kurita of Niigata University for reviewing the manuscript. Light microscope images of living specimens were taken by Mr. S. Machidori.

References

Anderson, O.R. and Bennett, P., 1985, A conceptual and quantitative analysis of skeletal morphogenesis in living species of solitary Radiolaria: *Euchitonia elegans* and *Spongaster tetras*. *Marine Micropaleontol.*, **9**, 441-454.

Anderson, O.R., Hemleben, C., Spindler, M. and Lindsey, J., 1986, A comparative analysis of the morphogenesis and morphometric diversity of mature skeletons of living *Didymocyrtis tetrathalamus tetrathalamus* and *Hexalonche amphisiphon*. *Marine Micropaleontol.*, **11**, 203-215.

De Wever, P., Sanfilippo, A., Riedel, W. R. and Gruber, B., 1979, Triassic radiolarians from Greece, Sicily and Turkey. *Micropaleontology*, **25**, 75-110.

Dumitrica, P., 1991, Middle Triassic Tripedurnulidae, n. fam. (Radiolaria) from the Eastern Carpathians (Romania) and Vicentinian Alps (Italy). *Rev. Micropaleont.*, **34**, 261-278.

Haeckel, E., 1887, Report on the Radiolaria collected by H.M.S. "Challenger" during the years 1873-1876. *Rept. Voy.* "*Challenger*"*, Zool.*, **18**, 1-1803.

Itaki, T., Matsuoka, A., Yoshida, K., Machidori, S., Shinzawa, M. and Todo, T., 2003, Late spring radiolarian fauna in the surface water off Tassha Aikawa Town, Sado, central Japan. *Sci. Rep., Niigata Univ., Ser. E (Geol.)*, no. 18, 41-51.

Kurihara, T. and Matsuoka, A., 2004, Shell structure and morphologic variation in *Spongosphaera streptacantha* Haeckel (Spumellaria, Radiolaria). *Sci. Rep., Niigata Univ., Ser. E (Geol.)*, no. 19, 35-48.

Matsuoka, A., 1992, Skeletal growth of a spongiose radiolarian *Dictyocoryne truncatum* in laboratory culture. *Marine Micropaleontol.*, **19**, 287-297.

Matsuoka, A., Shinzawa, M., Yoshida, K., Machidori, S., Kurita, H. and Todo, T., 2002, Early summer radiolarian fauna in surface waters off Tassha, Aikawa Town, Sado Island, central Japan. *Sci. Rep., Niigata Univ., Ser. E (Geol.)*, no. 17, 17-25.

Matsuoka, A., Yoshida, K., Hasegawa, S., Shinzawa, M., Tamura, K., Sakumoto, T., Yabe, H., Niikawa, I. and Tateishi, M., 2001, Temperature profile and radiolarian fauna in surface waters off Tassha, Aikawa Town, Sado Island, central Japan. *Sci. Rep., Niigata Univ., Ser. E (Geol.)*, no. 16, 83-93.

Petrushevskaya, M.G., 1968, Gomologii v skeletakh radiolyarii Nassellaria. 1. Osnovnye dugi v semeistve Cyrtoidea. *Zoologicheskii Zhurnal*, **47**, 1296-1310.

Sugiyama, K., 1993, Skeletal structures of Lower and Middle Miocene lophophaenids (Radiolaria) from central Japan. *Trans. Proc. Palaeont. Soc. Japan, N. S.*, no. 169, 44-72.

Swanberg, N.R. and Bjørklund, K.R., 1987, The pre-cephalic development of the skeleton of *Amphimelissa setosa* (Actinopoda: Nassellarida). *Marine Micropaleontol.*, **11**, 333-341.

Explanation of Plate 1

SEM images of radiolarian skeletons from sea water off Tassha, Sado Island. The scale bar of each figure equals 100μm.

1. *Neosemantis distephanus* Popofsky, ID number=926-2SD-5, 743-6-7.
2. *Neosemantis* ? sp., ID number=926-2SD-5, 743-5-7.
3. *Pseudocubus obeliscus* Haeckel, ID number=926-2SD-5, 741-4-5.
4. *Pseudocubus* sp. A, ID number=926-2SD-5, 743-6-1.
5. *Plectacantha* sp. A, ID number=926-2SD-5, 741-2-2.
6. *Plectacantha trichoides* Jørgensen, ID number=926-2SD-5, 741-3-9.
7. *Plectacantha* sp. B, ID number=926-2SD-5, 742-2-1.
8. *Plectacantha oikiskos* (Jørgensen), ID number=926-2SD-5, 742-3-2.
9. ?*Peridium longispinum* Jørgensen, ID number=926-2SD-5, 742-4-6.
10. *Plectacantha* ? sp., ID number=926-2SD-5, 742-3-1.

Plate 1

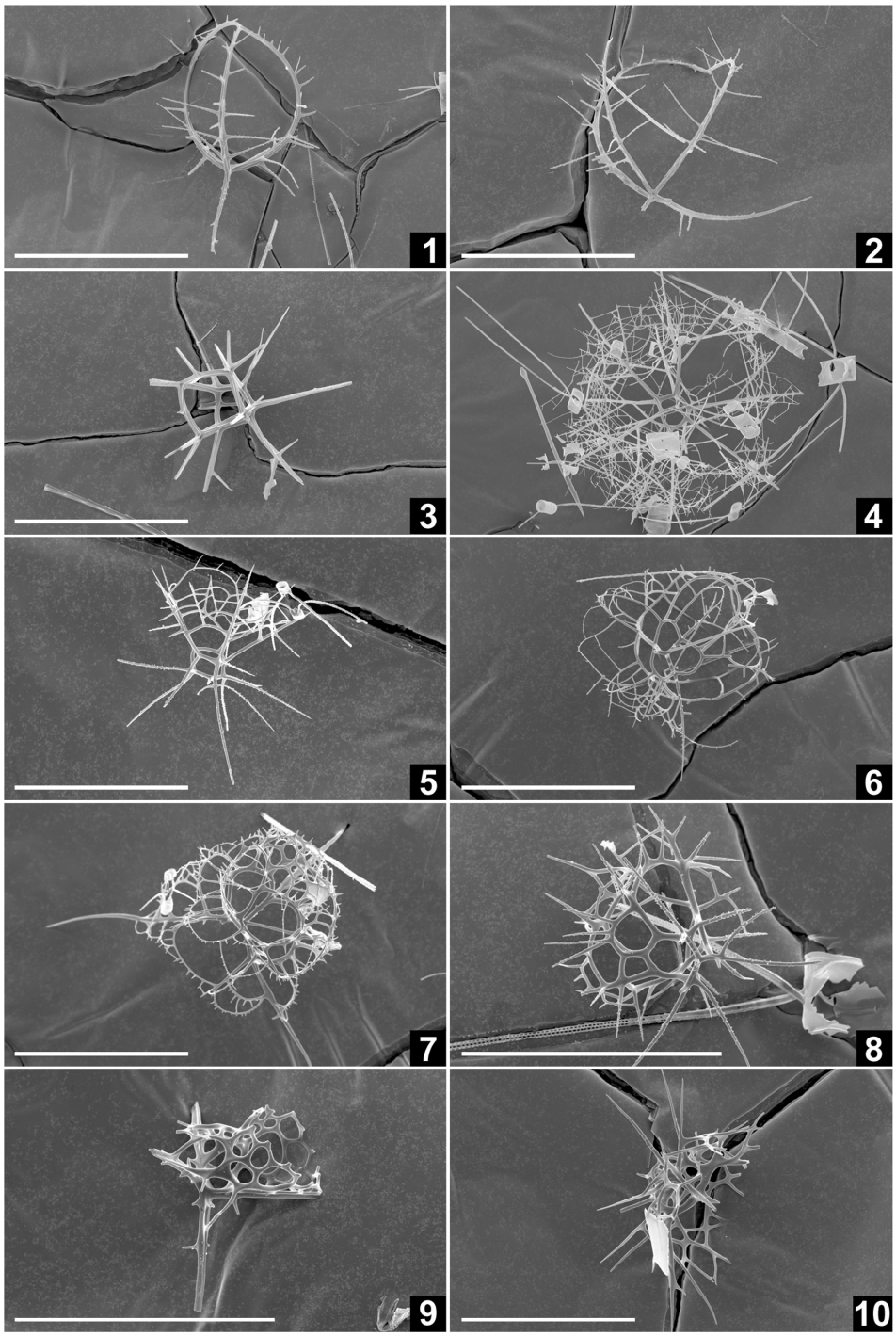

Explanation of Plate 2

SEM images of radiolarian skeletons from sea water off Tassha, Sado Island. The scale bar on each figure equals 100μm.

1. *Pseudodictyophimus gracilipes* (Bailey), ID number=926-2SD-5, 741-4-2.
2. *Phormacantha hystrix* (Jørgensen), ID number=926-2SD-5, 741-5-6.
3. *Litharachnium tentorium* Haeckel, ID number=926-2SD-5, 742-6-6.
4, 5. *Tetrapyle octacantha* Müller, 4: ID number=926-2SD-5, 743-5-3, 5: ID number=926-2SD-5, 741-5-3.
6. *Larcospina quadrangular* Haeckel, ID number=926-2SD-5, 742-6-7.
7. *Hexacontium* sp., ID number=926-2SD-5, 743-2-7.
8. *Spongosphaera streptacantha* Haeckel, ID number=926-2SD-5, 741-1-9.
9. *Dictyocoryne* sp., ID number=926-2SD-5, 742-4-7.
10. *Euchitonia* aff. *elegans* (Ehrenberg), ID number=926-2SD-5, 742-6-1.

Plate 2